transport for material repair. In order to achieve motion in such media, there are, however, two key challenges to address: rst the particle must overcome the e ect of con nement created by the surrounding material and second, motion must be triggered remotely since the particle cannot be accessed when located deep inside a porous medium. For this class of locomotion, telescoping peristaltic motion has been commonly observed among organisms such as maggots[28,29], and earthworms[30]. ese organisms generate an elongation wave along their body and establish directional frictional contact with the con ned surrounding using the ratcheted structure on their skin. In synthetic systems, such peristaltic deformation has been mimicked by a Belousov-Zhabotinsky reaction that periodically triggers the swelling/deswelling of a hydrogel particle[31,32]. is approach however did not produce enough deformation to enable e cient motion[33]. Yeghizarian and colleagues[4] later achieved motion with a hydrogel in a con ned tube by manually propagating volumetric phase transitions as a peristaltic wave along its body. In this approach, the hydrogel exhibited sustained motion similar to that of an earthworm, however, this system required manual and localized actuation and thus its potential may in practice be limited. e availability of e cient, remote controlled motile systems for porous media therefore remains an obstacle to the development of so actuators and drug delivery systems. In this study, we use inspiration from the crawling mechanics of maggots and larvae to develop a millimeter-size hydrogel particle (referred to as Mag-bot for “Magnetically Actuated Gel Bot”) that can crawl between two con ned plates and that is powered by a remote magnetic eld. While the proof of concept behind such as system was demonstrated in earlier work at the centimeter scale[34], the contributions of this work is three folds: (a) the mag-bot is magnetically actuated and can therefore be powered from a distance, (b) locomotion is enabled via the fabrication of a micron-sized scale pattern that has the potential of

with adhesive tapes. A er assembly, the con ned chamber was immersed in an aqueous surfactant (Tween 20) solution for lubrication. As shown in Fig. 2d, the structure of the scale-like micro-patterns can be characterized by two parameters: the tilt angle of the scales and the scale density. e tilt angle θ is de ned by the angle between the pattern and the vertical axis shown in Fig. 2d and accounts for the anisotropy of the scales. Under this de nition, $\theta = 45°$ corresponds to isotropic scales and $\theta \sim 90°$ corresponds to the most anisotropic structure. e scale density is measured by L_0/λ where λ is the distance between the two neighboring tilted scales (Fig. 2d) and L_0

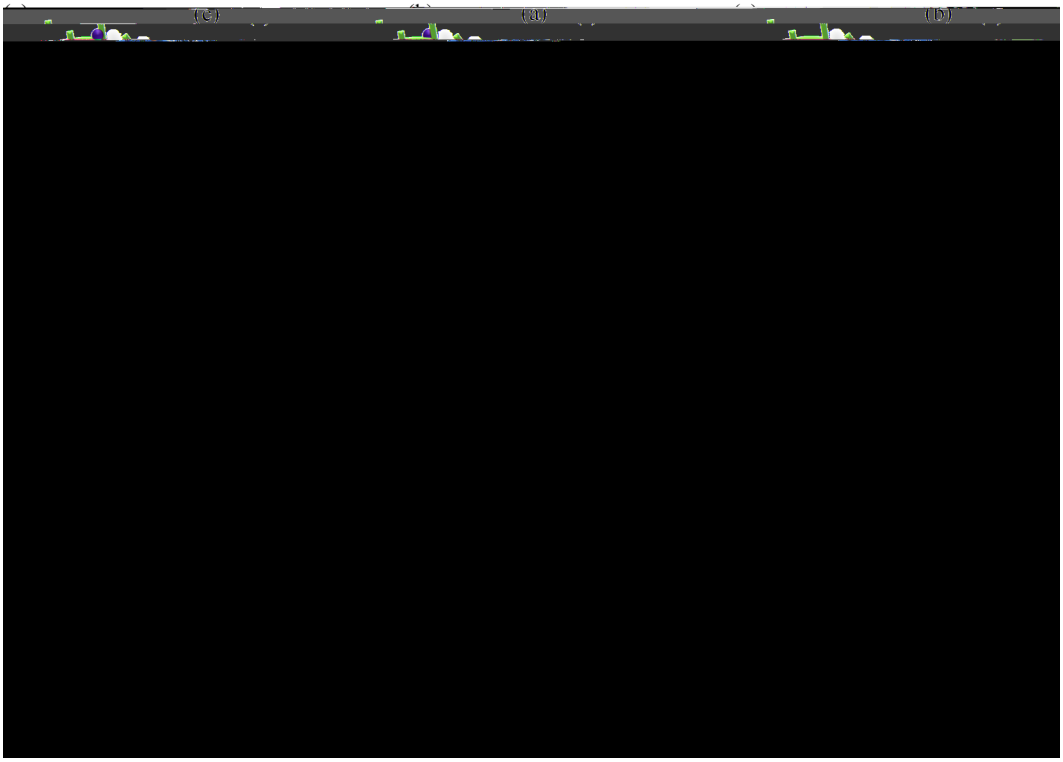

direction of lowest friction and particle motion. For instance, in Fig. 4a,c, we show ve sequential snapshots of a hydrogel particle that has been subjected to two deswelling-swelling cycles against surfaces characterized by di erent scale tilt angles. In Fig. 4a, the scales are isotropic, with tilt angle $\theta = 45°$, while in Fig. 4c, the scales are anisotropic, with tilt angle $\theta = 81°$.

As a result of the di erence in scales, the particle exhibit distinguished mobility on the scales. For isotropic scales (Fig. 4a), the particle gained zero e ective locomotion over the course of two cycles. However, for anisotropic scales (Fig. 4c), a clear directional migration towards the right (front) of the particles was observed. To connect this motion to deformation, we show the positions of the front (x_f) and back (x_b) edges of the particles, as well as the position x_c of their centroid as a function of cycle numbers in Fig. 4c. During the deswelling stages (i.e., ①-②), both particles contracted, during which front and back of the particle slid backward and forward, respectively. During the swelling stages (i.e., ③-④), the expansion of the particles occurred in a manner that was symmetric to the contraction stage, i.e., the front and back of the particle slid forward and backwards, respectively. In general, we observed that, for isotropic substrate, the forward sliding was equal to the backward sliding in both swelling and deswelling stages, resulting in zero e ective motion of the particle centroid; for anisotropic substrate, the forward sliding was greater than the backward sliding for the particles and thus its centroid moved continuously forward, whose step size per cycle is denoted by Δs.

Discussion

To better understand the relationship between particle deformation and motion, as well as the dependence of such parameters on the geometry of the micropatterned surfaces, we schematically depict the particle deformation along its principle direction in Fig. 5. It is convenient to introduce the so-called *Anchor Point* (AP), de ned as the point on the particle's surface that displays an e ective zero velocity during either the swelling or deswelling state. e location of this point is a hallmark of the substrate asymmetry and motion. Indeed, when the friction properties are symmetric (Fig. 5a), the AP is located at the particle's center and the deformation is fully symmetric during a deswelling-swelling cycle, yielding a zero e ective particle velocity. When the substrate friction is asymmetric, however, a greater portion of particle slides forward, such that the AP is located at the front of the particle during the deswelling stage (AP_d in Fig. 5b) and at the back of the particle during the swelling stage (AP_s in Fig. 5b). As a result of this biased deformation, the particle continuously moves towards the right with a displacement Δs.

To further elucidate the how the AP is shi ed by friction asymmetry and the e ect of this on particle's motion, we consider the mechanics of a long cylindrical particle (length, , cross-section, A,) elongated in a con ned chamber. For this, let us de ne a coordinate system (0,x) associated with the particle in its undeformed con guration. e longitudinal particle deformation can then be characterized by the displacement $u(x,t)$ and linearized

strain $\varepsilon = \partial u/\partial x = u_{,x}$ of points along the principle direction. To obtain a qualitative understanding, we use a linear Hookean constitutive law to approximate the mechanical behavior of the particle in the form $\sigma = Eu_{,x}$ where σ and E are the stress and Young's modulus of the gel, respectively. Note that a nonlinear hyperelastic constitutive model can be used for a more accurate characterization of stress-strain relationship as discussed in[34]. e frictional shear stress τ

$$EAu_{xx} - 2\mu b\sigma_n = 0. \tag{1}$$

Here, b is the width of the contact zone between the gel and the patterns. By directly integrating Eq. 1 in the domains on each side of the AP along the particle respectively and ensuring the continuity of strain at the AP, we can obtain a simple relationship between the position of the AP and the deformation of hydrogel as (derivation is provided in Supplemental Information I):

$$\alpha = \frac{^{+} - ^{-}}{^{+} + ^{-}} = \frac{1 - \Delta l^{-}/\Delta l^{+}}{1 + \Delta l^{-}/\Delta l^{+}}$$

Compared to available approaches for self-propelled particles, the possibility of powering motion with remote

7. Umetani, Y. & Hirose, S. Biomechanical Study of Serpentine Locomotion. In *On eory and Practice of Robots and Manipulators*, Springer Vienna, 1974, 171–184.
8. Dreyfus, R. *et al*. Microscopic arti cial swimmers. *Nature* **437**(7060), 862–865 (2005).
9. Mano, N. & Heller, A. Bioelectrochemical Propulsion. *J. Am. Chem. Soc.* **127**(33), 11574–11575 (2005).
10. Lozano, C., ten Hagen, B., Löwen, H. & Bechinger, C. Phototaxis of synthetic microswimmers in optical landscapes. *Nat. Commun.* **7**, 12828 (2016).
11. Howse, J. R. *et al*. Self-Motile Colloidal Particles: From Directed Propulsion to Random Walk. *Phys. Rev. Lett.* **99**(4), 048102 (2007).
12. Izri, Z., van der Linden, M. N., Michelin, S. & Dauchot, O. Self-Propulsion of Pure Water Droplets by Spontaneous Marangoni-Stress-Driven Motion. *Phys. Rev. Lett.* **113**(24), 248302 (2014).
13. Grančič, P. & Štěpánek, F. Active targeting in a random porous medium by chemical swarm robots with secondary chemical signaling. *Phys. Rev. E* **84**(2), 021925 (2011).
14. Lagubeau, G., Le Merrer, M., Clanet, C. & Quéré, D. Leidenfrost on a ratchet. *Nat. Phys.* **7**(5), 395–398 (2011).
15. Linke, H. *et al*. Self-Propelled Leidenfrost Droplets. *Phys. Rev. Lett.* **96**(15), 154502 (2006).
16. Benet, E. & Vernerey, F. J. Mechanics and stability of vesicles and droplets in con ned spaces. *Phys. Rev. E* **94**(6), 062613 (2016).
17.

Acknowledgements

We thank Dr. Kelsey Childress for help in preparing the hydrogels and Dr. Christopher Bowman for access to the alternating magnetic eld generator. Support from the National Science Foundation (DMR-1411320) is acknowledged.

Author Contributions